

Controlling the photoconductivity: Graphene oxide and polyaniline self assembled intercalation

Sesha Vempati, Sefika Ozcan, and Tamer Uyar

Citation: *Appl. Phys. Lett.* **106**, 051106 (2015);

View online: <https://doi.org/10.1063/1.4907260>

View Table of Contents: <http://aip.scitation.org/toc/apl/106/5>

Published by the [American Institute of Physics](#)

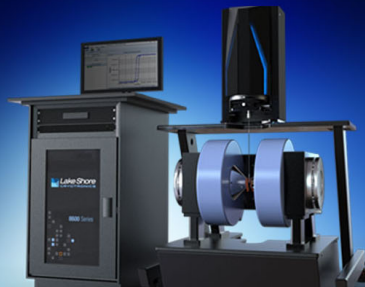
Articles you may be interested in

Publisher's Note: "Controlling the photoconductivity: Graphene oxide and polyaniline self assembled intercalation" [*Appl. Phys. Lett.* **106**, 051106 (2015)]

Applied Physics Letters **106**, 119902 (2015); 10.1063/1.4914864

[Fabrication and applications of multi-layer graphene stack on transparent polymer](#)

Applied Physics Letters **110**, 041901 (2017); 10.1063/1.4974457



8600 Series VSM

For fast, highly sensitive
measurement performance

LEARN MORE 

Controlling the photoconductivity: Graphene oxide and polyaniline self assembled intercalation

Sesha Vempati,^{1,a)} Sefika Ozcan,^{1,2} and Tamer Uyar^{1,3,b)}

¹UNAM-National Nanotechnology Research Centre, Bilkent University, Ankara 06800, Turkey

²Department of Polymer Science and Technology, Middle East Technical University, Ankara 06800, Turkey

³Institute of Materials Science and Nanotechnology, Bilkent University, Ankara 06800, Turkey

(Received 9 December 2014; accepted 21 January 2015; published online 4 February 2015; publisher error corrected 9 February 2015)

We report on controlling the optoelectronic properties of self-assembled intercalating compound of graphene oxide (GO) and HCl doped polyaniline (PANI). Optical emission and X-ray diffraction studies revealed a secondary doping phenomenon of PANI with –OH and –COOH groups of GO, which essentially arbitrate the intercalation. A control on the polarity and the magnitude of the photoresponse (PR) is harnessed by manipulating the weight ratios of PANI to GO (viz., 1:1.5 and 1:2.2 are abbreviated as PG1.5 and PG2.2, respectively), where $\pm PR = 100(R_{\text{Dark}} - R_{\text{UV-Vis}})/R_{\text{Dark}}$ and R corresponds to the resistance of the device in dark or UV-Vis illumination. To be precise, the PR from GO, PANI, PG1.5, and PG2.2 are +34%, –111%, –51%, and +58%, respectively.

© 2015 AIP Publishing LLC. [<http://dx.doi.org/10.1063/1.4907260>]

Graphene in its pure,^{1,2} doped,³ or heterocombination^{4,5} is proven to be potential in the context of photodetectors.⁶ It is of course convincing that the pristine graphene requires some sort of modification(s) to tune the properties or to exploit a synergy effect.^{6,7} Apart from the aforementioned modifications,^{1,3–5} graphene can form intercalating compound (GIC).^{7–11} GICs are more than 170 years old (Ref. 1 in Ref. 12) despite they still attract a lot of research attention^{8–11} due to their intriguing properties, such as unusual permeation,⁸ temperature dependent lattice expansion,^{10,11} controllable conduction type,⁷ superconductivity,⁷ are a few to mention. In a recent report,⁴ charge transfer is observed from C₆₀ to few layer graphene depicting a negative photoresponse (PR); however, here we report a simultaneous control on the polarity and magnitude through GICs. A list of intercalants can be identified, e.g., MeOH/EtOH/H₂O,^{8,10,11} acids,¹² and others⁷ (H, Au, Ge, etc). Interestingly, GICs with conducting polymers such as polyaniline are not largely seen^{13,14} apart from the composites,^{15–19} where the contribution of the polymer is unquestionable^{20,21} due to its electronic states,²² asymmetric charge conjugation,²³ and high doped-state-conductivity.²¹ GICs, apart from ground state electronic phenomenon (superconductivity⁷), they are mostly studied for local electronic information^{7,9} but not spatially averaged and excited state electronic behavior of macroscale devices which assesses their versatility.

Given the above background, graphene oxide (GO) and HCl doped polyaniline (PANI) were chosen to synthesize the intercalating compound (PGI), where kinetic formation efficiency of GO is better than graphite. The formation of PGI is self-controlled and mediated by the presence of ionic interactions, which is crucial for large scale synthesis of such compound materials. It is elucidated that PANI consists of emeraldine base and salt phases (EB and ES, respectively). In PGIs, the EB regions of PANI withdraw protons from

–OH/–COOH groups (of GO) which essentially manipulate the carrier density apart from the interplanar spacing (*d*) of GO, i.e., the present case is particularly different from the existing GICs as PANI interacts with GO through the functional groups. vis a vis alkali atoms are ionized and “dope” the graphene with their outer valence “s” electron.⁷ PR studies under UV-Vis illumination on GO, PANI, and PGIs suggest a hybrid response where polarity and magnitude are controllable. These results are well corroborated by the results from diffraction patterns and optical emission studies.

GO²⁴ and PANI²⁵ were synthesized as described in the literature. Transmission electron microscopy (TEM, FEI-Tecna G2 F30) images were obtained from dispersions of GO or PANI in deionized water. Initially, PANI is sonicated for 2–3 min to which GO is added to yield PANI:GO:1:1.5 (PG1.5) and PANI:GO:1:2.2 (PG2.2) ratios by weight and stirred for 5–7 h. Aqueous dispersions of GO and PANI were also prepared. X-ray diffraction (XRD) patterns were recorded (PANalytical X’Pert Pro with Cu K α radiation) on thoroughly dried samples. Each of the dispersions was dropcasted on cleaned ITO substrate and electrical contacts were obtained with conducting graphite paste. Essentially, ITO/GO, PANI, or PGI/ITO structures were investigated. Devices were illuminated (300 W, Ultra-Vitalux lamp, Osram) at a distance of ~30 cm from the source through ~10 cm of water column to eliminate the IR component. The *IV*-spectra were recorded with Keithley 4200 semiconductor characterization system. Emission responses were recorded from Horiba Scientific FL-1057 TCSPC at an excitation wavelength of ~300 nm and deconvoluted with OriginPro 8.5. Apart from the number of peaks, the other parameters were set as free until convergence, unless otherwise specified.

TEM images of GO and PANI are shown in Figs. 1(a) and 1(b), respectively. The exfoliated GO is explicit in contrast to its typical layered structure.²⁶ The implanted oxygenous groups (C–O, C=O, and O–C=O) hinder the attractive forces and separate the individual sheets in GO.^{13,24,26} It is interesting to note that PANI has also depicted sheet like

^{a)}svempati01@qub.ac.uk. Telephone: (+90) 3122903533

^{b)}uyar@unam.bilkent.edu.tr. Telephone: (+90) 3122903571

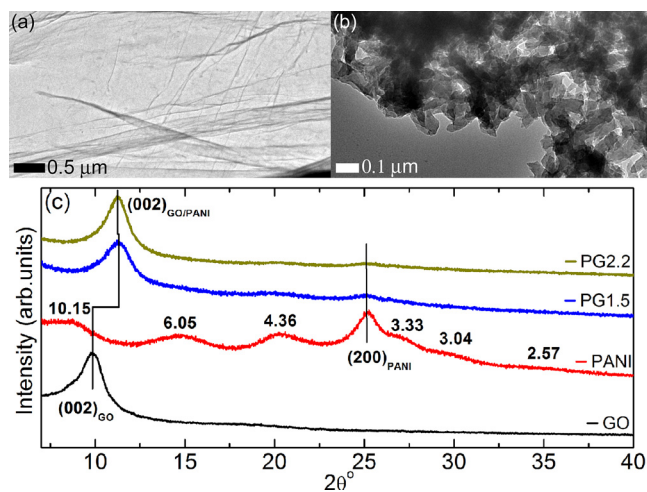


FIG. 1. TEM images of (a) GO, (b) PANI, and (c) XRD patterns from pristine GO, PANI, and PGIs. Long range ordering and lattice spacings from EB regions of PANI are annotated in Å.

structure (Fig. 1(b)) similar to the literature.¹⁸ XRD patterns from GO, PANI, and PGIs are shown in Fig. 1(c). GO exhibited a d of ~ 8.975 Å corresponding to $(002)_{GO}$. Notably, here the d is ~ 2.6 times higher^{13,24,26} than its unoxidized counterpart (not shown here). The XRD pattern from PANI exhibited multiple peaks; however, the overall crystal structure and the interplanar spacing depend on the solvent and degree of doping, respectively, i.e., the concentration ratio of $[Cl]/[N]$ in the case of HCl doping as in present case.²⁷ ES regions are conducting and crystalline in contrast to EB regions which are insulating, however, exhibit long range ordering (~ 10.15 Å at $2\theta = \sim 8.71^\circ$). Hence PANI is in fact a mixture of ES and EB,²⁷ which may fall under pseudorthorhombic lattice. Moving onto the PGIs, broadly PG1.5 and PG2.2 depicted a single well resolved feature at $2\theta = \sim 11.29^\circ$ apart from a signature of $(200)_{PANI}$. Notably, $(002)_{GO}$ is shifted to $\sim 11.29^\circ$ due to GO/PANI intercalation,¹² and we call this reflection as $(002)_{GO/PANI}$. Such shift is not observed in the earlier reports (Ref. 18 and Ref. 15 therein) which might be because of the differences in the synthesis process of GO,¹³ PANI, and PGIs. On contrary, a shift to smaller angle is observed in the context of GO/PANI composite.^{14,16,19} Note that d depends on the type of intercalant in the case of graphite as well.¹² It is more contextual to discuss the intercalation in the later part of this report after addressing the emission properties.

The emission response from GO, PANI, and PGI are shown in Fig. 2. Emission from PG1.5 is spectrally very similar to that of PG 2.2⁷ and hence the latter is considered for discussion. Nevertheless, the differences in their electronic properties are addressed with reference to the PR. It is notable that the origin of fluorescence from GO is of intense discussion, where the emission is attributed to the localized sp^2 clusters or oxygenous groups (Ref. 13, and references therein). In any case, the broad peak centered at ~ 545 nm consists of four bands⁷ of uncertain origin.¹³ For PANI, the emission exhibited two bands, viz., 388 nm and 440 nm. Quinoid groups in PANI are short lived excited states with no fluorescence.²⁸ Besides they act as traps and quench the fluorescence from adjacent benzenoid groups. Hence, the emission is a balance between benzenoid and quinoid groups.²⁰

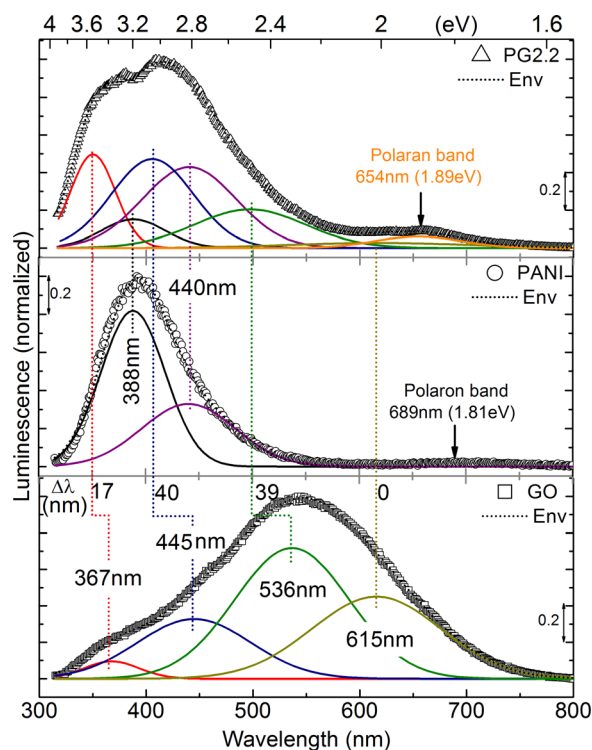


FIG. 2. Emission spectra of GO, PANI, and PG2.2. Spectral positions of various peaks are annotated. $\Delta\lambda$ -wavelength shift and Env-envelope of the simulated curves.

Overall, these features are similar to PANI in which a mixture of EB and ES regions is present. This is consistent with our XRD data and the literature.^{20,27} Also a very small emission is observed at ~ 1.81 eV which we believe to be originated from a transition to polaron band.^{22,23} When leucoemeraldine base (LEB) is oxidized no changes in the characteristics (fwhm and center of the peak) of the constituting peaks are observed.^{7,20} This is the basis for inputting fixed peak characteristics related to that of PANI⁷ while deconvoluting the emission from PG2.2. Since the intensity changes are inevitable²⁰ during the oxidation of PANI, the area under the peak is set as free until convergence. Understanding the interaction between PANI and GO is a prerequisite to comprehend the emission from PGI because of the following reasons. (a) In the XRD patterns of PGIs, the signal from EB is almost diminished while $(200)_{PANI}$ reflection from ES regions is still persistent (Fig. 1(c)). (b) PGI depicted a remarkable decrease in d of $\sim 13\%$ from pristine GO. Given the proton donating nature of $-OH$ and $-COOH$ groups of GO¹³ (with varying acidic strength²⁶), an interaction between the EB regions of PANI and GO is expected to form ES^* . This interaction initiates an intercalation process in the dispersion which is then settled upon solidification, where EB regions are relatively more functional than ES regions (in line with (a) and (b)). Similar to ES, ES^* regions also form a polaron band, however, at a slightly different energetic location within the band gap. The integral effect of ES and ES^* resulted a peak at 1.89 eV, where ES caused an emission band at 1.81 eV. From the deconvoluted peaks, a blue shift ($\Delta\lambda$, Fig. 2) of the emission bands is noticed with an exception for ~ 615 nm peak. The effective blue shift of peaks from GO is convincing,^{13,29} which is due to the deprotonation of $-OH$ and $-COOH$

groups. Furthermore, the emission bands related to PANI and GO were relatively extinguished (area under the peak) upon intercalation,⁷ which is rational^{13,30} as GO-COO^- is not fluorescent. GO sheets are electronically modified to a major extent by loosing protons and possible π - π interactions with PANI. Conspicuously, the present emission spectrum from PGI is in clear contrast to an earlier report.¹⁹

By taking together the analyses of XRD and emission spectra, an intercalated structure is confirmed. The effectiveness of the intercalation may be assisted by the slow evaporation (dropcasting) of the dispersion medium (H_2O), where a self-assembly is mediated by ionic interactions. It is expected that all of the GO sheets were intercalated as the $(002)_{\text{GO}}$ reflection is absent within the detection limits of XRD, while we note the possibility of formation of amorphous phase GO. The additional degree of freedom of benzene rings of PANI plays a critical role in the formation of PGI, where they can rotate/flip.^{23,27,31,32}

The IV -characteristics of GO, PANI, and PGI are shown in Fig. 3 along with the quantified $\pm\text{PR}\%$ [$=100(\text{R}_{\text{Dark}} - \text{R}_{\text{UV-Vis}})/\text{R}_{\text{Dark}}$], where R denotes the resistance of the device in dark or UV-Vis condition close to zero bias. Also $-ve$ or $+ve$ flag indicates increased or decreased “ R ” under illumination. In the following discussion, dark or UV-Vis condition are annotated with a suffix. Log-log plots were analyzed and the corresponding slopes and voltage regions are tabulated.⁷ For GO_{Dark} the charge transport is assisted by disrupted sp^2 conjugated network.^{26,33} While in $\text{GO}_{\text{UV-Vis}}$ case e/h pairs are created which effectively decrease the resistance ($+\text{PR}$) (Ref. 33 and Refs. 31–35 therein). However, computational studies on GO indicated the e -trapping ability of $\text{C}=\text{O}$ groups under excited state (e.g., UV-Vis light).³³ Consequently, the $+34\%$ PR of GO is a result of a competition between the “trapping” and “photogeneration.” GO_{Dark} depicted a slope of ~ 1.03 on log-log plot within the entire bias range which suggests an Ohmic conduction.⁷ Interestingly, $\text{GO}_{\text{UV-Vis}}$ depicted three

regions of different slopes on log-log scale, viz., 1.05 (0.02–1 V), 1.17 (1–5 V), and 0.76 (5–10 V). Although the first two slopes are not very different, the transition from 1.05 to 1.17 is evolved during the fitting process. The increase in slope can be attributed to the release of trapped charges^{26,33} while notably such change is not seen for GO_{Dark} device. At higher biases, the slopes drop down to 0.76 suggesting a current saturation.

In $\text{PANI}_{\text{Dark}}$, the conduction takes place via superposed quasi 1D and 3D variable range hopping models assisted by polarons or bipolarons^{21,34} as PANI is not charge conjugation symmetric.²³ Interestingly, $\text{PANI}_{\text{UV-Vis}}$ has shown $-\text{PR}$ for which two different attributions are noticed.^{35,36} (1) LEB regions trap the photogenerated charge carriers under green illumination.³⁵ This attribution is corroborated by the fact that LEB is transparent to green light where the e/h pairs are created in ES within the interface of LEB. Also the existence of equal amounts of LEB and pernigraniline base is suggested.³⁵ (2) ES is already in the polaronic state, further photo-oxidation can form pernigranil salt which is not a good conductor.³⁶ The suitability of these interpretations is addressed latter. Slopes from the IV -curves of $\text{PANI}_{\text{Dark}}$ and $\text{PANI}_{\text{UV-Vis}}$ on log-log scale are 1.01 (0.02–2 V) and 0.96 (0.02–2 V), respectively,⁷ which suggest almost no change in the conduction mechanism. However, the PR from PANI and GO of -111% and $+34\%$ are noteworthy.

In the case of PGIs, the conduction is mediated by GO, ES, and ES^* . After the deprotonation, electron density on GO sheet is slightly increased.²⁶ In contrast to other GICs in which alkali atoms are ionized and “dope” the graphene with their outer valence “ s ” electron.⁷ Besides, due to ES^* , the interfacial traps are also decreased within PANI, see (1). Hence, a bright signature of the individual components cannot be expected; however, a delicate balance is prompted in the PR. Apart from Fermi level equilibration, the density of total GO-trap centers ($\text{C}=\text{O}$) is invariant (ignoring the inaccessible) upon intercalation. Supposedly, PGI hosts charge traps from interfacial and/or other defects which exist even in dark condition.² Hence, the conduction in $\text{PG1.5}_{\text{Dark}}$ is due to the remaining charge carriers. Particularly, four regions of varying slopes are noticed on log-log scale for $\text{PG1.5}_{\text{Dark}}$, viz., 1.03 (0–1 V), 1.21 (1–2 V), 1.38 (2–6 V), and 1.16 (6–10 V).⁷ As the bias range increases, the slope of IV -curve on log-log scale also increases before settling at 1.16. The change in the slope can be attributed to the release of trap charges.²⁶ On the other hand, $\text{PG1.5}_{\text{UV-Vis}}$ depicted three different slopes of 1.02 (0–1 V), 1.13 (1–4 V), and 1.46 (4–10 V) on log-log plot. The slopes increase with bias range implies that current saturation may occur at much higher biases. Under illumination, $\text{C}=\text{O}$ groups from GO gain access to trap charge carriers; however, relatively higher voltages may be required to pull the electrons back into the conduction²⁶ and hence current saturation is not observed.

On log-log plot, $\text{PG2.2}_{\text{Dark}}$ depicted four regions of different slopes which are quite distinctive from that of $\text{PG1.5}_{\text{Dark}}$ viz., 4.83 (0–1 V), 1.88 (1–1.3 V), 0.86 (1.3–2.6 V) and 2.11 (2.6–10 V).⁷ As seen in $\text{PG1.5}_{\text{Dark}}$ case, the changes in the slopes are due to the release of trap charges, where an increase in ES^* regions should be noted. $\text{PG2.2}_{\text{UV-Vis}}$ depicted slopes of 4.13 (0–0.5 V), 1.12 (0.5–1 V), 0.73 (1–6 V), and 1.49 (6–10 V) on log-log scale which are quite different from

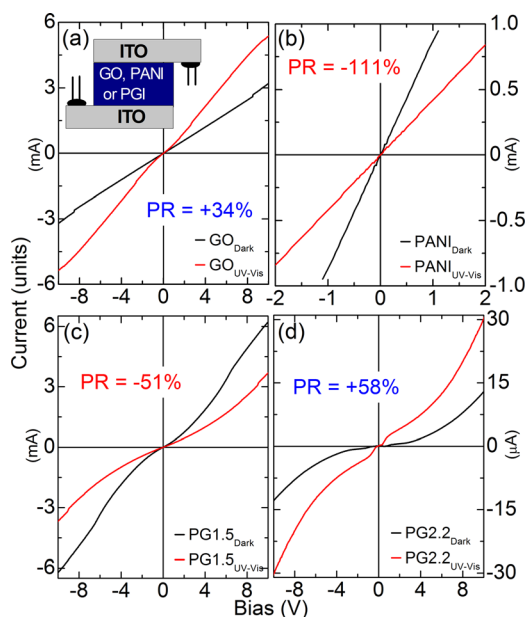


FIG. 3. IV -spectra of (a) GO, (b) PANI, (c) PG1.5, and (d) PG2.2 under dark and UV-Vis conditions. Inset of (a) shows the schematic of the device structure.

that of PG1.5_{UV-VIS}. For PG2.2 case, the density of EB regions is certainly decreased; however, lack of knowledge about the interfacial and other traps² hinders elaborate interpretation of the changes in the conduction behavior. The benzenoid rings of PANI can rotate/flip which significantly alter the electronic structure and electron-phonon interaction.^{23,27,31,32} This can be amplified in PGIs and complicates the conduction process further. Apart from the complexity involved with the second dopant (oxygenous groups of GO), the electrons trapped at the EB regions are confined to 1D (polymer chain) before they recombine with a hole or hop to a conducting region, viz., GO, ES, or ES*.

The PR of PG1.5 is -51% in sharp contrast to PG2.2 with $+58\%$ apart from the variations in the charge transport behavior with bias. In the following, a logical argument is provided enabling the appropriate interpretation of PR and controlling dynamics of the transformation of $-PR$ into $+PR$. If interpretation (2) is suitable when the doping level of PANI is increased (PG1.5 to PG2.2) then equivalently the density of ES* regions also increased. As a result, the $-PR$ should be more prominent. However, this is not the case as PG2.2 has shown $+PR$ of 58% . Therefore, in line with (1) when the doping level increased the EB regions were decreased, and consequently $+PR$ is reflected. Since the density of EB regions was not sufficiently decreased for PG1.5, it depicts $-PR$. Also, all of the EB regions of PANI are doped by oxygenous groups of GO and hence the trap centers (EB) are still expected. On the other hand, large increase in GO content might lead to collapse of the intercalating structure, as the special dynamics should favor the formation of ES*.

Electron microscopy suggested a well exfoliated and sheet like structure of GO and PANI, respectively. The analyses from XRD and emission spectra vindicate the formation of PGI-compound apart from the existence of ES and EB regions of PANI. Also the doping of EB regions with the protons from $-OH$ and $-COOH$ groups of GO supports the formation of PGI via self controlled ionic interactions. The broad emission peak from PG2.2 is consistent based on the following observations: (i) Intensity of the peaks from PANI is decreased due to the protonation, (ii) blue shifting and subdued intensity of peaks from GO is a signature of deprotonation, and (iii) integrated ES and ES* polaron band. The $+PR$ of GO is attributed to increased net charge carrier density under illumination and $-PR$ of PANI to trapping of charge carriers by EB regions. In the case of PGIs, the density of EB regions is decreased due to the ES* formation and the PR is either $+ve$ or $-ve$ depending on the GO and PANI weight ratios. The analyses of IV -spectra indicated the formation of interfacial/other traps. Accurate determination of the conduction mechanism requires further investigation such as temperature dependent IV -spectra; however, it is out of the scope of this letter. The polarity of the PR displayed is based on the balance between the charge generation against interfacial/other traps, EB regions of PANI, and excited state $C=O$ groups of GO. Finally, a control on the polarity and the magnitude of the PR in PGIs is wisely harnessed by manipulating the weight ratios of PANI to GO. The present nanoscale architecture will be potential in photodetectors and related optoelectronic applications.

S.V. thanks The Scientific and Technological Research Council of Turkey (TUBITAK) (TUBITAK-BIDEB 2221-

Fellowships for Visiting Scientists and Scientists on Sabbatical) for the postdoctoral fellowship. T.U. thanks The Turkish Academy of Sciences – Outstanding Young Scientists Award Program (TUBA-GEBIP) for partial funding.

- ¹T. Hosseini and N. A. Kouklin, *Appl. Phys. Lett.* **105**, 043104 (2014).
- ²A. Berholts, T. Kahro, A. Floren, H. Alles, and R. Jaaniso, *Appl. Phys. Lett.* **105**, 163111 (2014).
- ³J. Zhao, L. Tang, J. Xiang, R. Ji, J. Yuan, J. Zhao, R. Yu, Y. Tai, and L. Song, *Appl. Phys. Lett.* **105**, 111116 (2014).
- ⁴C. B. Flores, R. Y. Sato-Berrú, and D. Mendoza, *Appl. Phys. Lett.* **105**, 191116 (2014).
- ⁵T. Hosseini, D. Tomer, S. Rajput, L. Li, and N. Kouklin, *Appl. Phys. Lett.* **105**, 223107 (2014).
- ⁶F. H. L. Koppens, T. Mueller, Ph. Avouris, A. C. Ferrari, M. S. Vitiello, and M. Polini, *Nat. Nanotechnol.* **9**, 780 (2014).
- ⁷See supplementary material at <http://dx.doi.org/10.1063/1.4907260> for additional citations, emission spectra, deconvoluted peak characteristics, and slopes of IV -curves for different voltage regions.
- ⁸S. You, J. Yu, B. Sundqvist, L. A. Belyaeva, N. V. Avramenko, M. V. Korobov, and A. V. Talyzin, *J. Phys. Chem. C* **117**, 1963 (2013).
- ⁹M. Petrovic, I. S. Rakic, S. Runte, C. Busse, J. T. Sadowski, P. Lazic, I. Pletkovic, Z.-H. Pan, M. Milun, P. Pervan, N. Atodiresei, R. Brako, D. Sokcevic, T. Valla, T. Michely, and M. Kralj, *Nat. Commun.* **4**, 2772 (2013).
- ¹⁰S. You, S. Luzan, J. Yu, B. Sundqvist, and A. V. Talyzin, *J. Phys. Chem. Lett.* **3**, 812 (2012).
- ¹¹S. You, B. Sundqvist, and A. V. Talyzin, *ACS Nano* **7**, 1395 (2013).
- ¹²N. I. Kovtyukhova, Y. Wang, A. Berkdemir, R. Cruz-Silva, M. Terrones, V. H. Crespi, and T. E. Mallouk, *Nat. Chem.* **6**, 957 (2014).
- ¹³S. Vempati and T. Uyar, *Phys. Chem. Chem. Phys.* **16**, 21183 (2014).
- ¹⁴Y. F. Huang and C. W. Lin, *Polymer* **53**, 1079 (2012).
- ¹⁵Y. Liu, R. Deng, Z. Wang, and H. Liu, *J. Mater. Chem.* **22**, 13619 (2012).
- ¹⁶K. Zhang, L. L. Zhang, X. S. Zhao, and J. Wu, *Chem. Mater.* **22**, 1392 (2010).
- ¹⁷L. Wang, Y. Ye, X. Lu, Z. Wen, Z. Li, H. Hou, and Y. Song, *Sci. Rep.* **3**, 3568 (2013).
- ¹⁸X. Chen, F. Meng, Z. Zhou, X. Tian, L. Shan, S. Zhu, X. Xu, M. Jiang, L. Wang, D. Hui, Y. Wang, J. Lu, and J. Gou, *Nanoscale* **6**, 8140 (2014).
- ¹⁹S. Goswami, U. N. Maiti, S. Maiti, S. Nandy, M. K. Mitra, and K. K. Chattopadhyay, *Carbon* **49**, 2245 (2011).
- ²⁰J. Y. Shimano and A. G. MacDiarmid, *Synth. Met.* **123**, 251 (2001).
- ²¹V. J. Babu, S. Vempati, and S. Ramakrishna, *Mater. Sci. Appl.* **4**(1), 1 (2013).
- ²²S. Stafstrom, J. L. Bredas, A. J. Epstein, H. S. Woo, D. B. Tanner, W. S. Huang, and A. G. MacDiarmid, *Phys. Rev. Lett.* **59**(13), 1464 (1987).
- ²³R. P. McCall, J. M. Ginder, M. G. Roe, G. E. Asturias, E. M. Scherr, A. G. MacDiarmid, and A. J. Epstein, *Phys. Rev. B* **39**, 10174 (1989).
- ²⁴D. C. Marcano, D. V. Kosynkin, J. M. Berlin, A. Sinitskii, Z. Sun, A. Slesarev, L. B. Alemany, W. Lu, and J. M. Tour, *ACS Nano* **4**(8), 4806 (2010).
- ²⁵J. Stejskal, *Pure Appl. Chem.* **74**, 857 (2002).
- ²⁶S. Vempati, A. Celebioglu, and T. Uyar, *J. Mater. Chem. C* **2**, 8585 (2014).
- ²⁷J. P. Pouget, M. E. Jozefowicz, A. J. Epstein, X. Tang, and A. G. MacDiarmid, *Macromolecules* **24**, 779 (1991).
- ²⁸J. R. G. Thorne, J. G. Masters, S. A. Williams, A. G. MacDiarmid, and R. M. Hochstrasser, *Synth. Met.* **49–50**, 159 (1992).
- ²⁹Z. Qian, C. Wang, G. Du, J. Zhou, C. Chen, J. Ma, J. Chen, and H. Feng, *Cryst. Eng. Commun.* **14**, 4976 (2012).
- ³⁰J. L. Chen and X. P. Yan, *Chem. Commun.* **47**, 3135 (2011).
- ³¹J. M. Ginder, A. J. Epstein, and A. G. MacDiarmid, *Solid State Commun.* **72**, 987 (1989).
- ³²J. M. Ginder and A. J. Epstein, *Phys. Rev. B* **41**, 10674 (1990).
- ³³H. Chang, Z. Sun, Q. Yuan, F. Ding, X. Tao, F. Yan, and Z. Zheng, *Adv. Mater.* **22**, 4872 (2010).
- ³⁴V. I. Krinichnyi, *Appl. Phys. Rev.* **1**, 021305 (2014), and references therein.
- ³⁵D. M. Bubb, S. M. O'Malley, C. Antonacci, R. Belmont, R. A. McGill, and C. Crimi, *Appl. Phys. A* **81**, 119 (2005).
- ³⁶C. S. Ryoo, E. Y. Jeon, J. H. Kim, J. H. Rhee, and H. Lee, *Synth. Met.* **55–57**, 200 (1993).